

## Comparison of Integrated and Sequential Design Approaches for Fatigue Analysis of a Jacket Offshore Wind Turbine Structure

Ana Glisic<sup>1</sup>, Ngoc-Do Nguyen<sup>2</sup>, Peter Schaumann<sup>1</sup>

<sup>1</sup>Institute for Steel Construction, Leibniz Universitaet Hannover, ForWind, Germany

<sup>2</sup>DNV GL – Energy, Hamburg, Germany

### ABSTRACT

One of the most important criteria in the design of fixed offshore wind turbine structures is fatigue resistance. There is an unabated need for research in order to improve and optimize current design methods. There are mainly two approaches for structural analysis available in the offshore industry: the Integrated Design Approach (IDA) and the Sequential Design Approach (SDA). Within the IDA, the entire wind turbine, consisting of the jacket structure including tower and the rotor nacelle assembly (RNA), is considered as a unique system exposed to wind- and wave-induced loads in an aero-hydro-elastic solver. In SDA, the jacket structure is converted into a superelement and implemented into an aero-elastic solver, where it is expanded by an RNA in order to obtain the wind-induced interface loads. The obtained interface loads are used for further analysis in a more advanced offshore code, where the wave-induced loads are simulated. The fatigue damage of the relevant K-joint in the support structure is afterwards compared to the one obtained in terms of IDA. Apart from the judgement about advantages and disadvantages of both approaches, this work benefits from confirming the reliability and applicability of both approaches.

**KEY WORDS:** Offshore wind turbines, jacket structure, integrated design approach, sequential design approach, superelements, SESAM, Bladed.

### INTRODUCTION

Nowadays, with respect to environmental-friendly solutions for energy resources, energy production turns to renewable energy resources and the leading one is wind energy. Apart from the onshore wind farms, offshore wind industry marks significant growth in number of installations, farm sizes, turbine rated capacities, water depths and distance from shore. Complicated and expensive transport and installation is justified with a higher electricity output compared to onshore wind turbines, due to the higher rated capacities and the lower turbulence level in offshore conditions. Gradual exhaustion of the available sites for onshore installations and on the other hand wide available locations for potential sites are another reason that justifies the decision to go offshore.

Steel jackets are support structures employed for offshore wind turbines (OWTs) in deeper waters, due to the higher stiffness at the footprint

and the smaller surface facing the wave loads compared to the monopiles which are dominating the offshore wind turbines market (Seidel, 2016). Furthermore, when talking about the new OWT installations in the EU in year 2016, jackets have a significant increase to 12% of all OWTs installed, compared to the year 2015.

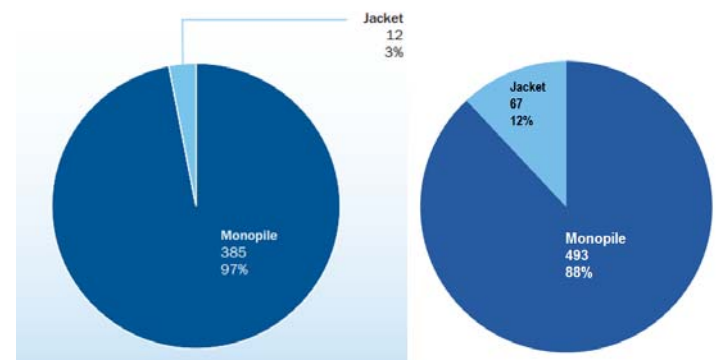


Fig. 1. Foundation types installed in 2015 (left) and 2016 (right) annual market

The general trend in the offshore wind turbine industry nowadays is increase of the maximum capacity, as shown in the Fig. 2. Recently, turbines with output of 10 MW have been installed, and in the future, sizes are expected to grow up to 20MW, if proven economically and technically feasible (The European Wind Energy Association EWEA, 2016; Wind Europe, 2017).

The size increase brings up the problem of larger generators, higher hub heights and larger structures and foundations, which leads to higher dynamic complexity of offshore wind turbines. As OWTs are exposed to cyclic aerodynamic, hydrodynamic and mechanical loading, they are especially prone to fatigue damage. This is a main design driving criteria, so continuous research and improvements are needed in the approaches for fatigue analysis. Two mainly used approaches in the industrial design are IDA and SDA with superelements.

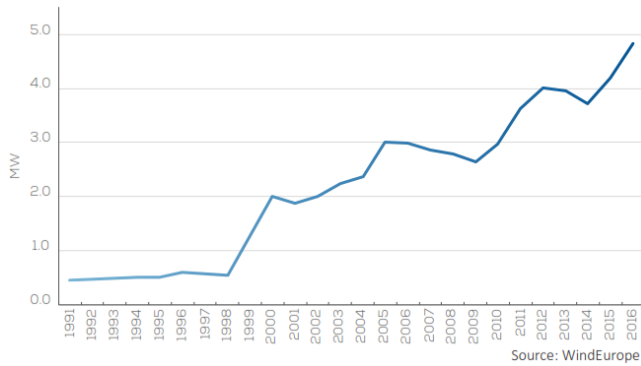


Fig. 2. Average offshore wind turbine rated capacity in MW

In the IDA, the whole system consisting of an entire wind turbine structure including jacket, tower and the RNA is exposed to wave-induced loads modelled as an irregular sea state by means of energy spectra and wind-induced loads modelled as turbulent wind fields. The complete design and simulations are carried out in the aero-elastic solver Bladed (detailed explanation in section Methods).

In SDA, the jacket structure is modelled in an advanced offshore code (SESAM) and implemented in an aero-elastic solver (Bladed) as a superelement. It is then expanded by an RNA in order to obtain the wind-induced interface loads. The obtained interface loads are used for further analysis back in SESAM, where the wave-induced loads are simulated. After the dynamic analysis is carried out, the fatigue damage of the corresponding K-joint in the jacket structure is obtained and compared to the one obtained in terms of IDA.

Although the SDA is more time consuming and some duplicated simulations must be carried out, it allows the foundation designer to share the design for aero-elastic analysis without needing to share the detailed jacket design with the wind turbine manufacturer. This criterion is often mandatory in the complex and multidisciplinary industrial design of OWTs.

## METHODS

### Integrated Design Approach (IDA)

The IDA workflow is shown in Fig. 3 (DNV-GL, 2016). First, the numerical model of the jacket structure is converted into a Bladed format and imported to Bladed (aero-elastic solver), where it is linked to a 10 MW wind turbine based on a realistic reference design (DNV-GL, 2017a; DNV-GL, 2017b; Dobbin, Cordle, Blonk, Langston, Kumar, Bossanyi, Vanni, de Batista, Hughes Salas and Davison, 2014).

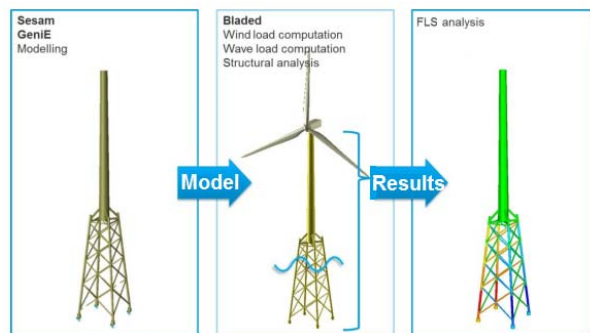


Fig. 3. Integrated design approach workflow when using Bladed (DNV GL, 2016)

### Numerical model

The jacket structure is designed for an offshore site with water depth of 50m. It is supported by four piles 40 m embedded in the soil, which are here modelled by means of springs with the equivalent stiffness (Phoon and Kulhawy, 1999). The footprint disposition is 34 x 34 m. The RNA has a rotor diameter of 178.16 m with a hub height of 118.38 m. The numerical Bladed model of the structure is shown in the Fig. 4.

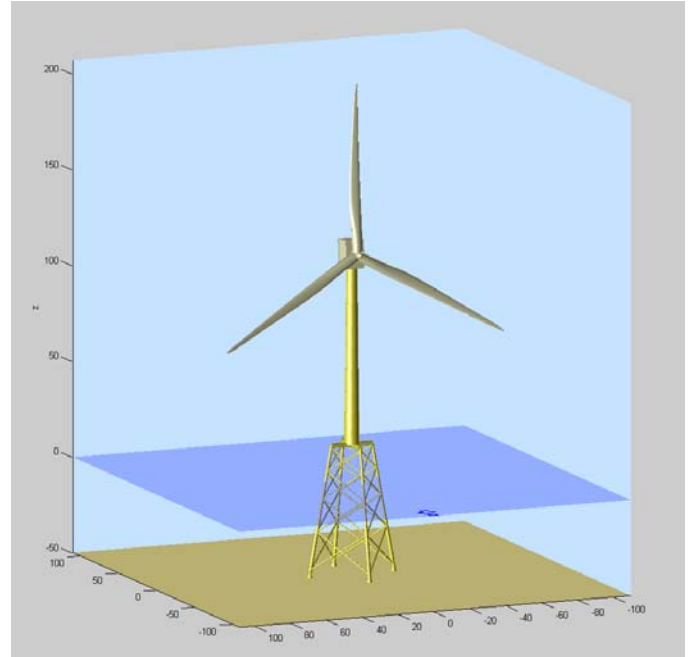


Fig. 4. Numerical 3D model of the jacket structure with tower and RNA in Bladed

### Loads

Wave loads are random and stochastic in shape, height, length and speed of propagation. In the literature (IEC 61400-3, 2008; DNV-RP-C203, 2016; Germanischer Lloyd, 2012; Böker, 2010; API 2A-WSD, 2000; Det Norske Veritas, 2007; Det Norske Veritas, 2014; Seidel, 2014 and other authors), many methods are proposed to describe and model the wave load conditions in the structural design. OWTs, as slender structures with a significant dynamic response, require stochastic modelling of the wave kinematics by means of irregular sea states. A sea state is defined by a wave-energy spectrum with a given significant wave height, a representative wave peak period, a mean propagation direction and a spreading function. Authors refer to Glisic et al., 2017 for a detailed explanation on modelling of irregular sea states in OWT design.

Regarding the realistic data, the mean wind speed for the target offshore site is 10 m/s (Fischer, de Vries and Schmidt, 2010). The wave energy spectra characteristics, namely significant wave height and mean zero-up crossing period, depend on the mean wind speed and in this case their values are respectively  $H_s=1.38$  m and  $T_z=3.87$  s. The irregular sea state is generated in Bladed and simulated 10 mins with a time step of 0.05 s. The whole process is repeated 6 times, each time changing only the randomness factor of the irregular sea state. That way, six different sea states with the same main characteristics are simulated and the fatigue damage is separately calculated for each simulation.

Wind loads are modelled by a turbulent wind field, where the basic idea is to describe spatial and temporal fluctuations with relevance for wind turbine load calculations. The turbulence has a three dimensional structure described by a spectral tensor. For a spectrum type, that describes the variance of the wind velocity fluctuations, Mann's model is chosen here, due to its good applicability for the flat, homogeneous terrains such as the sea surface. The main idea of this model is a division of the wind flow into a mean and a fluctuating part. For more detailed explanation about the Mann's model of the wind turbulence, authors refer to Mann, 1998.

The Bladed software has a subprogram that defines the wind turbulence, once having all the wind turbine input parameters (dimensions of the wind field that covers the whole rotor area, simulation duration, main wind speed, height where the main wind speed is captured – hub height). The defined turbulence is an output file (.wind file) of this subprogram. Afterwards it used as an input file that defines wind loads in the final wind-wave simulation. In the similar manner as for the wave loads, six simulations have been carried out. In each simulation, a different .wind file is used as a wind loads input file. Each of the six is created by the subprogram where the turbulence is defined with the same main characteristics, only the turbulence seed number is changed. Here, the fatigue damage is again separately calculated for each simulation.

To include the uncertainty caused by the stochastic nature of the wave and wind conditions, the final fatigue damage is taken as the mean value of the six separately calculated values.

The output of the simulations in Bladed are load time series. Comparing the loads in the members of the jacket structure, the most affected K-joint is chosen as the relevant one for this research. The most loaded K-joint is one the lowest four K-joints, as shown on the Figs. 5~6.

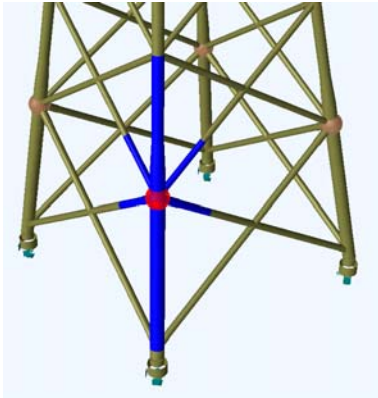


Fig. 5. The most loaded K-joint of the jacket structure

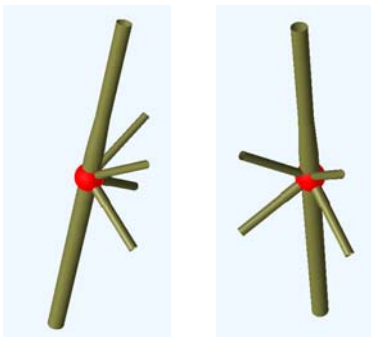


Fig. 6. Detail of the reference K-joint

Since the stress time series are needed for a fatigue damage calculation, stresses are calculated by a channel combination of load series, using the formulas from DNV GL-RP-C203, 2016. These formulas include the stress concentration factors (SCFs) for tubular joints, so those are calculated in terms of Eftymiou principle. It considers the geometry of the joint and the type of loads applied. For the K-joints, SCFs for tubular joints are calculated as given in the Appendix B of the DNV GL-RP-C203, 2016.

Once the SCFs, as well as the loads ( $F_x$ ,  $M_y$ ,  $M_z$ ), are known, the stresses of the reference K-joint are calculated in terms of hot spot stresses, using the Eqs 1~8. Fig. 6. (DNV GL-RP-C203, 2016) shows the hot spots locations on the brace circumference where the stresses are calculated, as well as the superposition of loads in the element in order to get the stresses. In each simulation, the highest of eight hot spot stresses is taken as the relevant one.

$$\sigma_1 = SCF_{AC}\sigma_x + SCF_{MIP}\sigma_{my} \quad (1)$$

$$\sigma_2 = \frac{1}{2}(SCF_{AC} + SCF_{AS})\sigma_x + \frac{1}{2}\sqrt{2} SCF_{MIP}\sigma_{my} - \frac{1}{2}\sqrt{2} SCF_{MOP}\sigma_{mz} \quad (2)$$

$$\sigma_3 = SCF_{AS}\sigma_x - SCF_{MOP}\sigma_{mz} \quad (3)$$

$$\sigma_4 = \frac{1}{2}(SCF_{AC} + SCF_{AS})\sigma_x - \frac{1}{2}\sqrt{2} SCF_{MIP}\sigma_{my} - \frac{1}{2}\sqrt{2} SCF_{MOP}\sigma_{mz} \quad (4)$$

$$\sigma_5 = SCF_{AC}\sigma_x - SCF_{MIP}\sigma_{my} \quad (5)$$

$$\sigma_6 = \frac{1}{2}(SCF_{AC} + SCF_{AS})\sigma_x - \frac{1}{2}\sqrt{2} SCF_{MIP}\sigma_{my} + \frac{1}{2}\sqrt{2} SCF_{MOP}\sigma_{mz} \quad (6)$$

$$\sigma_7 = SCF_{AS}\sigma_x + SCF_{MOP}\sigma_{mz} \quad (7)$$

$$\sigma_8 = \frac{1}{2}(SCF_{AC} + SCF_{AS})\sigma_x + \frac{1}{2}\sqrt{2} SCF_{MIP}\sigma_{my} + \frac{1}{2}\sqrt{2} SCF_{MOP}\sigma_{mz} \quad (8)$$

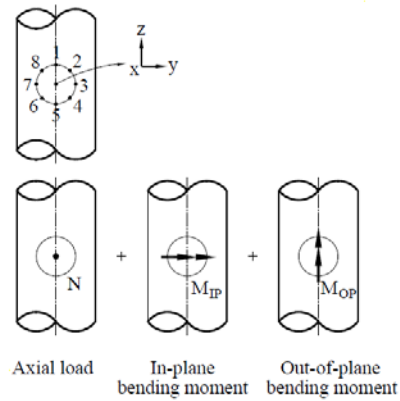


Fig. 6. Hot spots and superposition of loads in the K-joint

Now that the stress series for each of the six simulations are obtained, the next step for the fatigue calculation is to do a rainflow counting in order to get the number of cycles in the corresponding stress ranges. This is carried out using another subprogram in Bladed, which gives graphical and tabular interpretation of the rainflow counting results. The example for one of the six simulations is given in the Fig. 7.

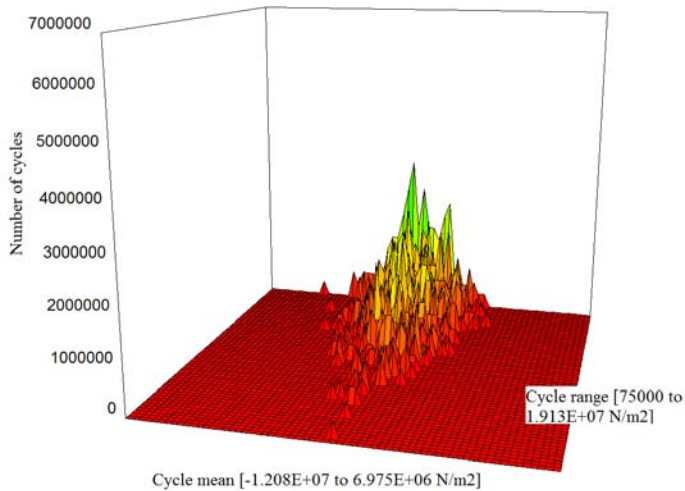


Fig. 7. 3D graphical interpretation of the rainflow counting

Once the rainflow counting is done and the number of cycles are attributed to the corresponding stress ranges, fatigue damage of the K-joint is calculated by means of Markov matrices (Guedes Soares, 2015). For the calculation of the fatigue damage, an S-N curve for the structures in the seawater with cathodic protection from DNV GL-RP-C203 is used (Fig. 8).

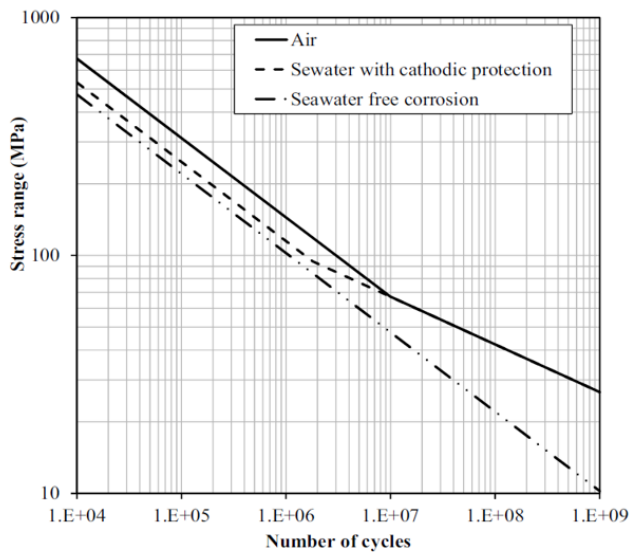


Fig. 8. S-N curves for tubular joints in air and sea water with cathodic protection (DNV GL, 2016)

As mentioned, the final fatigue damage that represents the IDA is taken as a mean value of six fatigue damages obtained through six simulations where the random factor of the irregular sea state and turbulence seed number took six different values. The fatigue damage is shown and compared with the one obtained in the SDA in the section Results.

### Sequential Design Approach (SDA)

The SDA workflow is shown in Fig. 9 (DNV-GL, 2016; Collier, 2016).

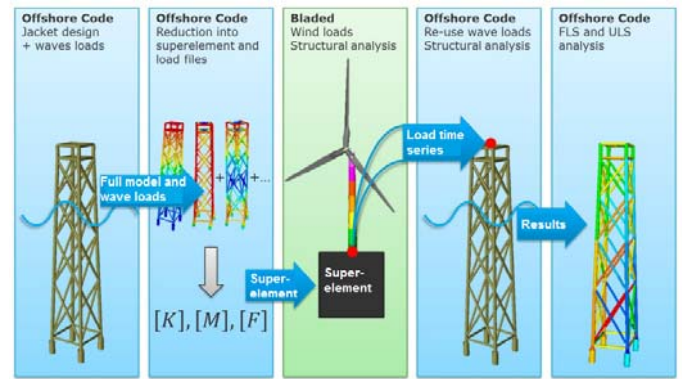


Fig. 9. Superelement sequential design approach workflow when using Bladed (DNV GL, 2016)

First, the numerical model of the jacket structure is developed in SESAM (hydro-elastic solver) and converted to a superelement. The superelement feature allows importing a reduced jacket model from a detailed offshore structural modelling software (here SESAM) into other aero-elastic solvers (here Bladed). In Bladed, it is expanded by a tower with an RNA. That way, the dynamic response of the jacket with an RNA (whole system) can be obtained in Bladed without an explicit structural model of the jacket defined in Bladed (Fig. 10). The key advantage of the SDA is that foundation designers can share their design for aero-elastic analysis without needing to share the jacket design details with the wind turbine designer/manufacturer (DNV GL, 2016).

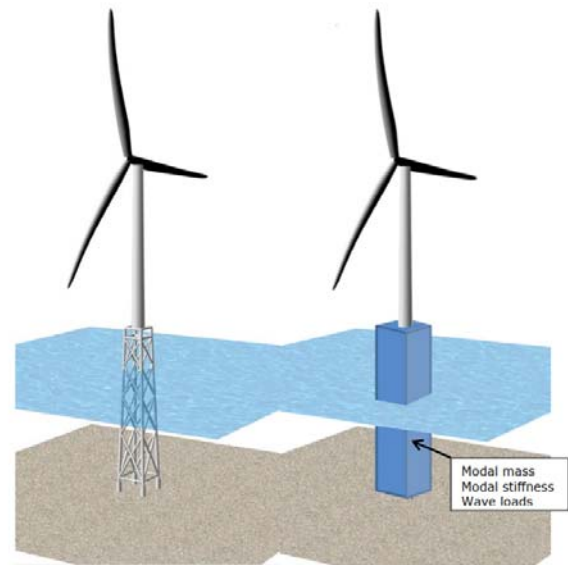


Fig. 10. Superelement representation replaces jacket model with modal information (DNV GL, 2016)

### Superelement model

The SESAM numerical FE model of the jacket structure is almost the same as the one in Bladed, explained in the IDA section. Furthermore, the jacket model from the IDA is developed in SESAM and then converted into Bladed format and implemented into Bladed for the IDA

simulations. The difference in this model is that it also contains a tower and a point mass that represents RNA (Fig. 11).

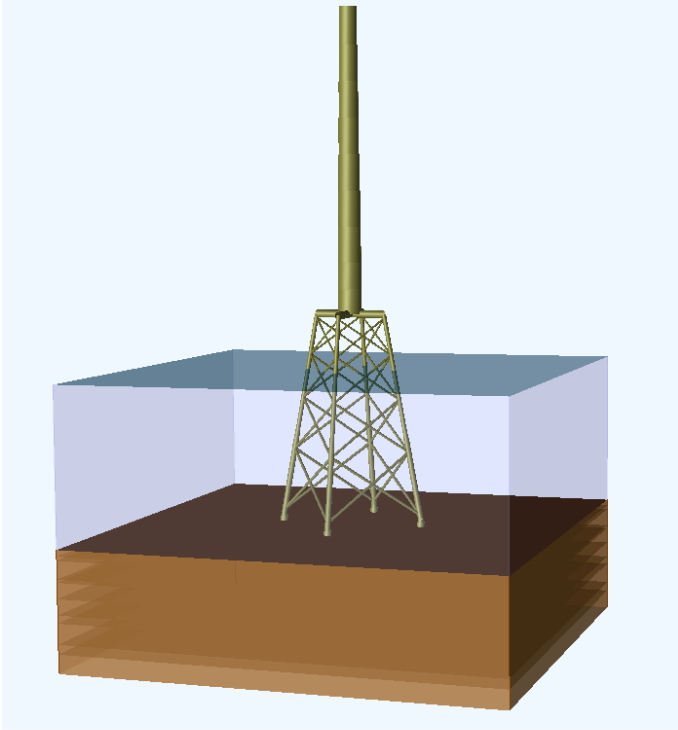


Fig. 11. Numerical 3D model of the jacket structure with a tower in SESAM

The SESAM model of the jacket is cut at the transition piece (interface node), and converted into a superelement in terms of Craig-Bampton method, that retains the accurate dynamic response of the jacket (Craig, 2000). A key concept is the division of the jacket nodes to the boundary node and the interior nodes. The boundary node is the interface node where the superelement connects to the tower base and the interior nodes are all other nodes in the jacket.

Craig-Bampton modes for the superelement consist of constraint and normal mode shapes. Constraint modes describe the displacement of the interior jacket nodes when six unit displacements (three translational and three rotational) are applied at the superelement interface (boundary) node. These mode shapes provide the static response of the superelement and allow the superelement interface node to move. For the normal modes, the jacket structure is constrained both at the base and at the interface node, so the modes include motion of the interior nodes only (that is why they are also called interior modes). The normal (interior) modes enhance the dynamic response of the superelement. The union of these two sets of modes provide an accurate dynamic model of the jacket and motion of the interface node.

The IDA that was carried out in Bladed also included damping. In order to make a reliable comparison between IDA and SDA, all possible sources of deviation should be removed. The available input option to include damping also in SDA is Rayleigh damping. In order to achieve in SESAM in SDA the same damping ratios for corresponding natural frequencies as in Bladed in IDA, Rayleigh's damping parameters  $\alpha$  and  $\beta$  are calculated for a desired damping ratio, using the Eq. 9:

$$\alpha + \beta\omega_i^2 = 2\omega_i\xi_i \quad (9)$$

where the:

$\omega_i$  is natural frequency,

$\xi_i$  is desired damping, taken from Bladed,

$\alpha, \beta$  – Rayleigh's damping parameters.

The superelement is now implemented in Bladed without its real physical interpretation, but with the modal information only (stiffness and mass matrices). The superelement's response is therefore close to that of the fully modelled jacket, up to a certain frequency. The model is upgraded in Bladed by adding the tower with an RNA and the wind loads are applied. Since the jacket is reduced to a superelement and contain no information about the detailed design, Bladed shows the upgraded model as a floating tower with an RNA (Fig. 12).

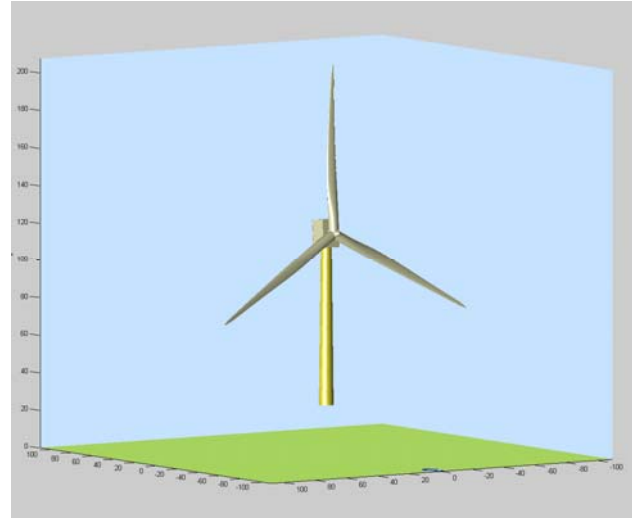


Fig. 12. Tower definition for superelement simulation in Bladed

#### Loads

The wind load simulation setup is the same like in the IDA. Again, six simulations have been conducted with different turbulence seeds. A feature of the SESAM software, named Fatigue Manager, is developed for the superelement operations manipulation and the fatigue calculation. Using this feature, in each Bladed wind load simulation, a .wind file has been saved that represents wind loads transferred to the interface node and will later be used in the final fatigue damage calculation.

Once the simulations in Bladed are carried out and wind load files obtained, the full jacket model with the tower is implemented into the SESAM's Fatigue Manager. The wave loads simulations set up is the same as in the IDA section, in terms of irregular sea state with the identical energy spectra characteristics ( $H_s, T_z$ ). For the wind loads, program now calls the .wind files obtained from Bladed. Wind and wave loads are again simulated for 10 mins with the time step of 0.05s. It is very important that the time step used in SESAM is equal to the one used in Bladed, in which the interface loads are received. If not, aliasing in the interface loads might result in incorrect results.

Further fatigue damage calculation is done in the Fatigue Manager, whereby all the input parameters are equal to those in the IDA. The fatigue damage is calculated for the same reference K-joint as in the IDA. The equal SCFs for the K-joint as in the IDA are considered. Once again, the final fatigue damage that represents the SDA is taken as a mean value of six fatigue damages obtained through six

simulations where the random factor of the irregular sea state and turbulence seed number took six different values.

### SUPERELEMENT CONVERGENCE

Before a result comparison can be performed, a verification is needed whether the created superelement model is valid. This is done by comparing it to the full model from the IDA. The verification requirements relate to spectral convergence and spatial convergence.

#### Spectral convergence

The standalone jacket mode shapes of the superelement model are compared to the full standalone jacket model (by standalone, it is meant only the jacket model up to the transition piece, without the tower). For the full jacket model, SESAM software is used to obtain the eigenfrequencies. Obtaining the eigenfrequencies of the superelement model requires reducing a full model to a superelement without using any time domain loads. The number of mode shapes included in the superelement can be adjusted until spectral convergence is reached. For the model at hand, the number of included mode shapes was increased from 20 until the satisfying convergence is obtained at 70 included mode shapes (76 degrees of freedom). The comparison between first 10 modes is shown in the Table 1.

Table 1. Natural frequencies of the standalone jacket for the full model and superelement model including 70 modes (76 DOFs)

Mode	Full model		Superelement		Rel. error
	Freq.[Hz]	Period [s]	Freq.[Hz]	Period [s]	Freq. [%]
1	0.732	1.366	0.734	1.362	0.27
2	0.732	1.366	0.734	1.362	0.27
3	1.379	0.725	1.614	0.620	14.56
4	1.379	0.725	1.614	0.620	14.56
5	2.031	0.492	2.661	0.376	23.68
6	2.369	0.422	2.745	0.364	13.79
7	2.563	0.390	3.745	0.267	31.56
8	2.563	0.390	3.867	0.259	33.72
9	2.577	0.388	4.659	0.215	44.69
10	2.735	0.366	4.676	0.214	41.51

Table 1 shows that in higher modes some differences in the eigenfrequencies of the full and reduced jacket model can be observed. This can be solved by including more modes in the superelement. This would also improve the accuracy for the lower modes, since the reduced structure would have more degrees of freedom. However, since these modes have very high frequency (over 10 Hz), no further mode shapes are included here.

#### Spatial convergence

The spatial convergence is verified by running a selection of load cases on both full and reduced (superelement) model. Comparing the structural analysis results in both files gives an idea about how well the superelement model is spatially converged.

In this case, the compared value in the structural analysis is the displacement of the interface point. It has been compared between the full model run in the direct time integration and the superelement conversion in the time domain including 40 modes. The displacements

in all load cases are very similar. The result of one of the load cases is shown in the Fig. 13.

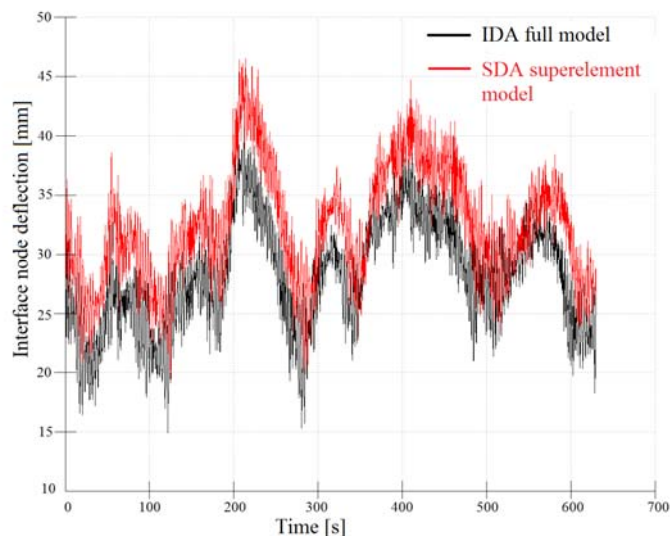


Fig. 13. Comparison of interface node deflection of the full and reduced model

As the Fig. 13 shows, the deviations between the displacements of the full and superelement model are less than 5 mm. Therefore, the spatial convergence is successfully verified.

### RESULTS

Now that all the simulation are carried out and the superelement model proved to be valid, final fatigue damages of the reference K-joint can be compared between IDA and SDA. Once again it is noted that for each approach six simulations are carried out, and the representative fatigue damage is the mean value. The results, as well as their comparison through relative error is shown in Fig. 14.

#### FATIGUE DAMAGE COMPARISON INTEGRATED Vs SEQUENTIAL APPROACH

INTEGRATED	
Simulation	Damage
1	1.36
2	1.23
3	0.97
4	1.05
5	1.08
6	1.62

Final damage: 1.22

The difference: 24.63%

SEQUENTIAL	
Simulation	Damage
1	1.29
2	1.98
3	1.61
4	1.85
5	1.54
6	1.43

Final damage: 1.62

Fig. 14. Fatigue damage comparison between IDA and SDA

The final result of comparing the two final fatigue damages of the IDA and SDA showed a difference of 24,6%, which is a satisfying accuracy, due to the stochastic nature of the processes included, the complexity of the algorithm and the fact that it is a deviation in the long term fatigue damage estimation. Although many steps are taken to overcome the differences in the details of calculations in these two approaches, there are some remained. The considered differences include:

- coordinate system transformations, as the coordinate systems between SESAM and Bladed are not compatible,
- including the damping parameters in SESAM, as they are automatically included in Bladed,
- including weight of marine growth and flooded members in both approaches
- defining the same time steps in the simulations in Bladed and SESAM.

The next steps in this research should increase the accuracy by:

- decreasing the amount of the information lost in the reduced model,
- including the Wheeler's stretching in modelling of the wave loads in the IDA (IEC 61400-3, 2008)

However, it is noted that the most of the accuracy-increasers also increase the computational time, which is in this research also relatively high (approximately 42 mins pro 10 min wind-wave simulation). Therefore, primarily is to define the purpose of the calculations. Depending on whether the focus is on the higher accuracy for sensitive researches or on the shorter computational time for some preliminary studies, one can balance the accuracy-increasers with the computational time.

## CONCLUSIONS

The purpose of the present study was to examine both approaches (integrated design approach IDA and sequential design approach SDA) in detail and get an insight about the advantages and disadvantages of both approaches. It is also a verification study to verify the conversion of the numerical model from SESAM into a superelement in Bladed. This study also addresses the sources of deviations in the results. Here, some of the differences were unavoidable due to the different starting assumptions in the software and limitations in the SESAM to Bladed converter. In total, the most important differences are related to geometric stiffening, structural damping and wave load modelling. This would be possible to improve through detailed case-sensitive changes directly in the software code.

The key advantages of the IDA are that it has a higher computational efficiency, it makes a aero-hydro-elastic coupling between the structure and wind/waves, it can include the non-linear features (such as soil springs) and the overall system optimization is easier in the IDA.

However, in the complex and multidisciplinary industrial design of OWTs, the use of the superelements is sometimes unavoidable, due to the data protection. Although the SDA requires time domain simulation in both Bladed and SESAM and therefore involves some duplication of simulation, it is sometimes necessary to use it in order not to share the detailed jacket design of the foundation designer with the wind turbine designer. SDA also benefits from the possibility to include some complex structural elements in the superelement, such as shell elements, which are normally not supported in Bladed. This way, Bladed gets only the information of the dynamic response of the jacket including such elements, runs the simulations and gets the accurate results.

The SDA is a new approach and it still needs to be validated in detail. Some basic validation is done in this study by comparing it to a commonly used IDA. Apart from that, this work also benefits from confirming the reliability and applicability of both approaches.

## ACKNOWLEDGEMENTS

The authors acknowledge with thanks the support of the European Commission's Framework Program "Horizon 2020", through the Marie Skłodowska-Curie Innovative Training Networks (ITN) "AEOLUS4FUTURE - Efficient harvesting of the wind energy" (H2020-MSCA-ITN-2014: Grant agreement no. 643167).

## REFERENCES

- API 2A-WSD (RP 2A-WSD), 21<sup>st</sup> edition (2000). "Recommended Practice for Planning, Designing and Constructing Fixed Offshore Platforms—Working Stress Design", *Recommended Practice*, American Petroleum Institute.
- Böker, C (2010). "Load simulation and local dynamics of support structures for offshore wind turbines", *PhD thesis, Leibniz Universität Hannover*.
- Collier, W (2016). "Superelement Beta: User Guide for Bladed 4.8", *DNV-GL, Doc. No. 110052-UKBR-T-27-F*.
- Craig, R (2000). "Coupling of substructures for dynamic analysis: an overview", *AIAA-2000-1573*.
- Det Norske Veritas (2014). "Design of offshore wind turbine structures", *DNV Offshore Standard*, DNV-OS-J101.
- Det Norske Veritas (2007). "Environmental conditions and environmental loads", *Recommended Practice*, Høvik, Norway DNV-RP-C20.
- DNV-GL (2016). "Fatigue design of offshore steel structures", *Recommended Practice*, DNV-RP-C203.
- DNV-GL (2017). "Implementing an interface between Bladed and Sesam - Verification report of Sesam's Bladed interface", *Report No. 2016-0866, Rev.1*.
- DNV-GL (2017). "Performing FLS and ULS analysis on fixed offshore wind turbine support structures in the time domain – Integrated design approach", *User course SESAM*.
- DNV-GL (2017). "Performing FLS and ULS analysis on fixed offshore wind turbine support structures in the time domain – Sequential and Superelement analysis approach", *User course SESAM*.
- Dobbin, J, Cordle, A, Blonk, L, Langston, D, Kumar, A, Bossanyi, E, Vanni, F, de Batista, M, Hughes Salas, O, Davison, F (2014). "Fully Integrated Design: Lifetime Cost of Energy Reduction for Offshore Wind", *The Proceedings of the 24th (2014) International Ocean and Polar Engineering Conference, ISOPE 14*.
- IEC 61400-3 Ed. 1, Wind Turbines – Part 3 (2008). "Design Requirements for Offshore Wind Turbines", *International Electrotechnical Commission (IEC)*.
- Fischer, T, de Vries, W and Schmidt, B (2010). "Upwind Design Basis (WP4: Offshore Foundations and Support Structures)", *Endowed Chair of Wind Energy (SWE) at the Institute of Aircraft Design, University Stuttgart*.
- Germanischer Lloyd (2012). "Rules and Guidelines", *IV Industrial Services: Guideline for the Certification of Offshore Wind Turbines, Hamburg*.
- Glisic, A, T. Ferraz, G, Schaumann, P (2017). "Sensitivity analysis of monopiles' fatigue stresses to site conditions using Monte Carlo Simulation", *The Proceedings of the 27th (2017) International Ocean and Polar Engineering Conference, ISOPE 17, San Francisco, USA*.
- Guedres Soares, C, Yeter, B, garbatov, Y (2015). "Fatigue damage assessment of fixed offshore wind turbine tripod support structures", *Engineering Structures, Volume 101, pp.518-528*.
- Mann, J (1998). "Stochastic wind loads on structures. Lecture notes", *Risø National Laboratory*.

Phoon, K-K and Kulhawy, FH (1999). "Characterization on geotechnical variability", *Canadian Geotechnical Journal*, 36, 612-624.

Seidel, M (2014). "Wave induced fatigue loads", *Stahlbau, Volume 83*, pp.535-541.

Seidel, M, Voormeeren, S, van der Steen, J (2016). "State-of-the-art design processes for offshore wind turbine support structures", *Stahlbau, Volume 85, Issue 9 (9/2016)*, Ernst & Sohn Verlag für Architektur und technische Wissenschaften GmbH & Co. KG, Berlin.

The European Wind Energy Association EWEA (2016). "Wind in power: 2015 European statistics", *Annual statistics 2016*

Wind Europe (2017). "The European offshore wind industry: *Key trends and statistics 2016*".